High Accuracy Numerical Methods for Parabolic Systems in Air Pollution Modelling

Venelin Todorov[1,2] Ivan Dimov[1] Juri Kandilarov[3] Lubin Vulkov[3]

[1]Department of Parallel Algorithms, Institute of Information and Communication Technologies, Bulgarian Academy of Sciences (IICT-BAS), Acad. G. Bonchev 25 A, 1113 Sofia, Bulgaria

[2]Department of Information Modelling, Institute of Mathematics and Informatics, Bulgarian Academy of Sciences (IMI-BAS), Acad. Georgi Bonchev Str., Block 8, 1113 Sofia, Bulgaria

[3] Rousse University "Angel Kanchev", Ruse, Bulgaria

Budapest, Hungary, November 28, 2019

Outline of the talk

- Introduction
- The Two Dimensional Model Problem of Air Pollution
- Central Difference Schemes and Richardson Extrapolation - Second-order space semidiscretization, Full discretization, Richardson extrapolation
- Compact Difference Schemes - Space discretization, Time discretization.
- Numerical results
  - Example 1 (Test problem with known analytical solution)
  - Example 2 (unknown exact solution)
- CONCLUDING REMARKS

The Two Dimensional Model Problem of Air Pollution

There has been growing interest of developing and using highly accurate numerical schemes for solving partial differential equations, leading to renewed interest in high-order compact difference schemes.
Compact schemes, proposed by Kreiss and Oliger use similar stencil, but requires a scalar tridiagonal or pentadiagonal matrix inversion. In this paper we use another idea. We employ high-order compact schemes, namely, we deal with the auxiliary relations yielded from the original differential equations by its differentiation in order to decrease the truncation error.
The simulation of various processes in chemistry, physics and engineering uses models of systems of coupled parabolic problems. In this work we construct compact high-order finite difference schemes for semilinear parabolic systems and propose fast algorithms for solution of the nonlinear algebraic equations. Problems of air pollution transport with coupling in the nonlinear reactions terms are of our main consideration, namely,

$$\frac{\partial u_l}{\partial t} - K\triangle u_l + \mathbf{b}_l \nabla u_l = R_l(x, y, u_1, \ldots, u_L), \quad (x, y, t) \in \Omega \times (0, T], \tag{1}$$

$$\mathbf{u} = 0, \quad (x, y, t) \in \partial\Omega \times (0, T], \tag{2}$$

$$\mathbf{u} = \mathbf{u}_0(x, y), \qquad (x, y) \in \Omega, \tag{3}$$

where $\mathbf{u} = (u_1, u_2, ..., u_L)$, $u_l = u_l(x, y, t)$, $l = 1, ..., L$ are the concentrations of L chemical species (pollutants) and $K > 0$ is the diffusion coefficient and $\Omega \in R^2$ is a bounded domain. The assumption regarding constant $K := K_x = K_y$ is not a restriction for developing our numerical approach. This just corresponds to the physical model described in several papers.

The main goal of the paper is the application and numerical illustration of above-mentioned difference approximations to the following real-life parabolic transport system. The advection part in (1) may be presented in the following form:

$$\mathbf{b_l}.\nabla u_l = \mu(y - y_c)\frac{\partial u_l}{\partial x} + \mu(x_c - x)\frac{\partial u_l}{\partial y}, \tag{4}$$

where $x \in (0, X)$, $y \in (0, Y)$, $x_c = X/2$, $y_c = Y/2$ and $\mu = 2\pi/T$. The nonlinear chemical part of the model is:

$$\begin{aligned}
R_1(u_1, ..., u_{10}) &= k_5 u_2 - (k_6 u_5 + k_4 u_7 + k_3 u_8)u_1, \\
R_2(u_1, ..., u_{10}) &= (k_6 u_5 + k_4 u_7 + k_3 u_8)u_1 - (k_5 + k_9 u_9)u_2, \\
R_3(u_1, ..., u_{10}) &= -k_1 u_3 u_9, \\
R_4(u_1, ..., u_{10}) &= 2k_1 u_3 u_9 + k_3 u_1 u_8 - k_2 u_4, \\
R_5(u_1, ..., u_{10}) &= k_2 u_5 \\
R_6(u_1, ..., u_{10}) &= k_9 u_2 u_9, \\
R_7(u_1, ..., u_{10}) &= 2k_2 u_4 + k_3 u_1 u_8 + k_{10} u_9 - k_4 u_1 u_7, \\
R_8(u_1, ..., u_{10}) &= 4k_1 u_3 u_9 - k_3 u_1 u_8, \\
R_9(u_1, ..., u_{10}) &= k_4 u_1 u_7 + 2k_8 u_{10} - (k_1 u_3 - k_9 u_2 + k_{10})u_9, \\
R_{10}(u_1, ..., u_{10}) &= k_7 u_5 - k_8 u_{10}.
\end{aligned} \tag{5}$$

This is a simplified chemical scheme, that will be used in most of the numerical experiments. It is rather simple (only 10 species are involved in this scheme), but all types of chemical reactions that are difficult for the numerical methods (non-linear chemical reactions and photochemical reactions) are represented in it. Therefore numerical methods that perform well in the treatment of this scheme should be expected to perform also well in the treatment of more complicated chemical schemes. Some of the coefficients belong to photochemical reactions (the ones with term $h\nu$), which means that these reactions depend on the light, more precisely on the position of the Sun relative to the horizon: in k_2, k_5 and k_7 the angle θ denotes the solar zenith angle, which is the angle of the Sun measured from vertical.

Table: The chemical reactions of the model

1	$HC + OH \rightarrow 4RO_2 + 2ALD$	6	$NO + O_3 \rightarrow NO_2 + O_2$
2	$ALD + h\nu \rightarrow 2HO_2 + CO$	7	$O_3 + h\nu \rightarrow O_2 + O(^1D)$
3	$RO_2 + NO \rightarrow NO_2 + ALD + HO_2$	8	$O(^1D) + H_2O \rightarrow 2OH$
4	$NO + HO_2 \rightarrow NO_2 + OH$	9	$NO_2 + OH \rightarrow HNO_3$
5	$NO_2 + h\nu \rightarrow NO + O_3$	10	$CO + OH \rightarrow CO_2 + HO_2$

Table: The chemical species in the model

u_1	u_2	u_3	u_4	u_5	u_6	u_7	u_8	u_9	u_{10}
NO	NO_2	HC	ALD	O_3	HNO_3	HO_2	RO_2	OH	$O(^1D)$

Table: The rate coefficients of the chemical reactions

k_1	$6.0e-12$	k_6	$1.6e-14$
k_2	$7.8e-05.\exp(-0.87/\cos\theta)$	k_7	$1.6e-04.\exp(-1.9/\cos\theta)$
k_3	$8.0e-12$	k_8	$2.3e-10$
k_4	$8.0e-12$	k_9	$1.0e-11$
k_5	$1.0e-02.\exp(-0.39/\cos\theta)$	k_{10}	$2.9e-13$

From both the practical and mathematical point of view, one is naturally interested in the existence and qualitative of the solutions to the problem (1)-(5). The well-posedness of initial boundary value problems for a system more general than (1) is obtained in [**?**]. Throughout of the rest of the paper we assume existence and uniqueness of classical solution of problem (1)-(5) which means a function that belongs to $C([0,T]\times\overline{\Omega})\bigcap C^1((0,T);C(\overline{\Omega}))\bigcap(C(0,T);C^2(\overline{\Omega}))$ and satisfies the equations (1)-(3) pointwise. Moreover, at the finite difference approximations we assume the existence of the fourth in time and the sixth in space derivatives.
Since we are interested in systems describing chemical concentrations, the *nonnegativity* of the solutions has to be preserved. It is proved, that if:

1.
$$\mathbf{u}_0(x,y)\geq 0; \tag{6}$$

2.
$$R_l(x,y,\mathbf{u}),\ l=1,...,L \tag{7}$$

is Lipshitz continuous with respect to the concentrations $u_1,u_2,\ldots,u_L$ and it satisfies the inequality
$$R_l(x,y,\mathbf{u})\geq 0, \tag{8}$$

whenever $u_l=0$, and
$$\mathbf{u}\in R_+^L\equiv\{u_k\geq 0,\ k=1,...,L\}, \tag{9}$$

then
$$\mathbf{u}\geq 0 \tag{10}$$

for all $(x,y)\in\Omega$ and $t\in[0,T]$.
It is easy to check that the chemical reactions $R_l(u_1,u_2,\ldots,u_{10})$, $l=1,...,10$ given by (5) satisfy the point 2. and the solution of problem (1)-(3) with (5) is nonnegative in time $t>0$ if the initial data
$$\mathbf{u}_0(x,y)\geq 0. \tag{11}$$

Central Difference Schemes and Richardson Extrapolation

In this section, for clarity exposition we describe the construction of the second order CDS for the weakly coupled system of two equations

$$\frac{\partial u}{\partial t} - a(x,y)\frac{\partial^2 u}{\partial x^2} - b(x,y)\frac{\partial^2 u}{\partial y^2} + c(x,y)\frac{\partial u}{\partial x} + d(x,y)\frac{\partial u}{\partial y} = r(x,y,t,u,v), \quad (12a)$$

$$\frac{\partial v}{\partial t} - e(x,y)\frac{\partial^2 v}{\partial x^2} - f(x,y)\frac{\partial^2 v}{\partial y^2} + g(x,y)\frac{\partial v}{\partial x} + h(x,y)\frac{\partial v}{\partial y} = s(x,y,t,u,v), \quad (12b)$$

defined on the cylindric domain $Q_T = \Omega \times (0, T]$, where $\Omega \subset R^2$ is a bounded domain with Lipshitz boundary. The nonlinear functions r and s are sufficiently smooth of their arguments. The coefficients $a(x,y)$, $b(x,y)$, $e(x,y)$ and $f(x,y)$ are positive in Ω. We consider Dirichlet boundary conditions

$$u(x,y,t) = \bar{\phi}(x,y,t), \quad v(x,y,t) = \bar{\bar{\phi}}(x,y,t), \quad (x,y,t) \in \partial\Omega \times (0,T] \quad (13)$$

and initial conditions

$$u(x,y,0) = \bar{\psi}(x,y), \quad v(x,y,0) = \bar{\bar{\psi}}(x,y), \quad (x,y) \in \Omega, \quad (14)$$

where $\bar{\phi}$, $\bar{\bar{\phi}}$, $\bar{\psi}$ and $\bar{\bar{\psi}}$ are given and smooth data and compatibility of the boundary and initial data is ensured.

Let for simplicity the domain Ω being a rectangle $\Omega = [0, X] \times [0, Y]$. We introduce uniform meshes in the following way:

$$\overline{\omega}_{h,x} = \{x_i = ih_x, \quad i = 0, 1, \ldots, M_x, \quad h_x = X/M_x\} \tag{15}$$

,

$$\overline{\omega}_{h,y} = \{y_j = jh_y, \quad j = 0, 1, \ldots, M_y, \quad h_y = Y/M_y\} \tag{16}$$

and then

$$\overline{\Omega}_h = \overline{\omega}_{h,x} \times \overline{\omega}_{h,y}, \tag{17}$$

$$\overline{\Omega}_h = \Omega_h \cup \partial\Omega_h, \tag{18}$$

where Ω_h consists of all interior mesh points and $\partial\Omega_h$ - of all boundary mesh points. We will use the index pair (i, j) to represent the mesh point (x_i, y_j) and define

$$u_{i,j} = u(x_i, y_j, t), \quad v_{i,j} = v(x_i, y_j, t), \quad r_{i,j} = r(x_i, y_j, t, u_{i,j}, v_{i,j}), \quad \text{ect.} \tag{19}$$

For $w = u, v$ we introduce the central difference operators

$$\begin{aligned} \delta_x w_{i,j} &= (w_{i+1,j} - w_{i-1,j})/(2h_x), & \delta_x^2 w_{i,j} &= (w_{i+1,j} - 2w_{i,j} + w_{i-1,j})/h_x^2, \\ \delta_y w_{i,j} &= (w_{i+1,j} - w_{i-1,j})/(2h_y), & \delta_y^2 w_{i,j} &= (w_{i,j+1} - 2w_{i,j} + w_{i,j-1})/h_y^2. \end{aligned} \tag{20}$$

Application of the difference operators (20) to the system (12) for $(i, j) \in \Omega_h$ leads to

$$\frac{du_{i,j}}{dt} - a_{i,j}\delta_x^2 u_{i,j} - b_{i,j}\delta_y^2 u_{i,j} + c_{i,j}\delta_x u_{i,j} + d_{i,j}\delta_y u_{i,j} + \chi_{i,j,1} = r_{i,j}, \tag{21}$$

$$\frac{dv_{i,j}}{dt} - e_{i,j}\delta_x^2 v_{i,j} - f_{i,j}\delta_y^2 v_{i,j} + g_{i,j}\delta_x v_{i,j} + h_{i,j}\delta_y v_{i,j} + \chi_{i,j,2} = s_{i,j}, \tag{22}$$

where the truncation errors $\chi_{i,j,1}$ and $\chi_{i,j,2}$ are

$$\begin{aligned} \chi_{i,j,1} &= \frac{h_x^2}{12}\left(2c\frac{\partial^3 u}{\partial x^3} - a\frac{\partial^4 u}{\partial x^4}\right)_{i,j} + \frac{h_y^2}{12}\left(2d\frac{\partial^3 u}{\partial y^3} - b\frac{\partial^4 u}{\partial y^4}\right)_{i,j} + \mathcal{O}(h_x^4 + h_y^4), \\ \chi_{i,j,2} &= \frac{h_x^2}{12}\left(2g\frac{\partial^3 v}{\partial x^3} - e\frac{\partial^4 v}{\partial x^4}\right)_{i,j} + \frac{h_y^2}{12}\left(2h\frac{\partial^3 v}{\partial y^3} - f\frac{\partial^4 v}{\partial y^4}\right)_{i,j} + \mathcal{O}(h_x^4 + h_y^4). \end{aligned} \tag{23}$$

After dropping the truncation error terms the semi-discrete second-order central difference approximation of (12) is obtained:

$$\begin{aligned} \frac{du^h_{i,j}}{dt} - a_{i,j}\delta_x^2 u^h_{i,j} - b_{i,j}\delta_y^2 u^h_{i,j} + c_{i,j}\delta_x u^h_{i,j} + d_{i,j}\delta_y u^h_{i,j} &= r^h_{i,j}, \\ \frac{dv^h_{i,j}}{dt} - e_{i,j}\delta_x^2 v^h_{i,j} - f_{i,j}\delta_y^2 v^h_{i,j} + g_{i,j}\delta_x v^h_{i,j} + h_{i,j}\delta_y v^h_{i,j} &= s^h_{i,j}, \end{aligned} \tag{24}$$

where for $(i,j) \in \Omega_h$

$$u^h_{i,j} \approx u(x_i, y_j, t), \qquad v^h_{i,j} \approx v(x_i, y_j, t), \tag{25}$$

$$r^h_{i,j} \approx r(x_i, y_j, t, u^h_{i,j}, v^h_{i,j}), \qquad s^h_{i,j} \approx s(x_i, y_j, t, u^h_{i,j}, v^h_{i,j}). \tag{26}$$

Now we introduce the matrix representation for the system (24). We order the mesh points lexicographically from left to right in x direction and from the bottom to the top in y direction. Excluding the boundary mesh points $(i,j) \in \partial\Omega_h$, for $j = 1, 2, ..., M_y - 1$ we define the following $(M_x - 1)$ dimensional vectors:

$$U^h_j = \left(u^h_{1,j}, u^h_{2,j}, ..., u^h_{M_x-1,j}\right), \qquad V^h_j = \left(v^h_{1,j}, v^h_{2,j}, ..., v^h_{M_x-1,j}\right), \tag{27}$$

$$R_j(U^h_j, V^h_j) = \left(R_{1,j}, R_{2,j}, ..., R_{M_x-1,j}\right), \qquad S_j(U^h_j, V^h_j) = \left(S_{1,j}, S_{2,j}, ..., S_{M_x-1,j}\right) \tag{28}$$

and then

$$U = \left(U^h_1, U^h_2, ..., U^h_{M_y-1}\right)^T, \qquad V = \left(V^h_1, V^h_2, ..., V^h_{M_y-1}\right)^T, \tag{29}$$

$$R = \left(R_1, R_2, ..., R_{M_y-1}\right)^T, \qquad S = \left(S_1, S_2, ..., S_{M_y-1}\right)^T. \tag{30}$$

We then rewrite the system (24) as a system of ODEs in matrix (vector) form

$$\frac{d}{dt}U + \bar{P}U = R + \bar{\Phi}, \quad t \in (0, T], \tag{31}$$

$$\frac{d}{dt}V + \bar{\bar{P}}V = S + \bar{\bar{\Phi}}, \quad t \in (0, T] \tag{32}$$

with initial conditions $U(0)$ and $V(0)$ obtained from $\bar{\psi}$ and $\bar{\bar{\psi}}$ for $(i,j) \in \Omega_h$ after the reordering. In (31) the matrix $\bar{P}$ is $(M_y - 1) \times (M_y - 1)$ block-tridiagonal matrix $\bar{P} = tridiag(\bar{P}_{k,k-1}, \bar{P}_{k,k}, \bar{P}_{k,k+1})$ and $\bar{P}_{k,l}$, $l = k-1, k, k+1$ are tridiagonal matrices for $l = k$ and diagonal for $l = k \pm 1$ of order $(M_x - 1) \times (M_x - 1)$. Let for two natural numbers m and M, $m < M$ denote $m : M = m, m+1, ..., M$ and assume that $\mathbf{p}_{k,m:M}$ is a vector with entrances $\mathbf{p}_{k,m:M} = (p_{k,m}, p_{k,m+1}, ..., p_{k,M})$. Then from (24) and (20) the entrances of $\bar{P}_{k,l}$ are

$$\bar{P}_{k,l} = tridiag(\mathbf{p}^{(-1,\varepsilon)}_{k,2:M_x-1}, \mathbf{p}^{(0,\varepsilon)}_{k,2:M_x}, \mathbf{p}^{(1,\varepsilon)}_{k,1:M_x-2}) \qquad l = k + \varepsilon, \;\; \varepsilon = 0, \pm 1\,, \tag{33}$$

where

$$\begin{aligned} p^{(\pm 1,0)}_{i,j} &= \pm\frac{c(i,j)}{2h_x} - \frac{a(i,j)}{h_x^2}\,, \\ p^{(0,\pm 1)}_{i,j} &= \pm\frac{d(i,j)}{2h_y} - \frac{b(i,j)}{h_y^2}\,, \\ p^{(0,0)}_{i,j} &= 2\frac{a(i,j)}{h_x^2} + 2\frac{b(i,j)}{h_y^2}\,. \end{aligned} \tag{34}$$

In fact, $\bar{P}$ is a matrix with global dimension $(M_x - 1)(M_y - 1) \times (M_x - 1)(M_y - 1)$. Replacing $a \leftrightarrow e$, $b \leftrightarrow f$, $c \leftrightarrow g$ and $d \leftrightarrow h$ in a similar way we obtain the entrances of the matrix $\bar{\bar{P}}$. The vectors $\bar{\Phi}$ and $\bar{\bar{\Phi}}$ in (31)-(32) are associated with the boundary functions and also depend on time t.

For discretization in time the so called θ-weight method is used. Let $\omega_\tau = \{t_n = n\tau, \quad n = 0, 1, \ldots, N, \quad \tau = T/N\}$ be uniform mesh in time with time step τ. Then the weight θ-discretization of (31), (32) may be written in the following way:,

$$\begin{aligned} \frac{U^{n+1} - U^n}{\tau} + \bar{P}U^{n,\theta} &= R^{n,\theta} + \bar{\Phi}^{n,\theta}, \quad t \in (0, T), \\ \frac{V^{n+1} - V^n}{\tau} + \bar{\bar{P}}V^{n,\theta} &= S^{n,\theta} + \bar{\bar{\Phi}}^{n,\theta}, \quad t \in (0, T), \end{aligned} \tag{35}$$

where $Z^{n,\theta} = \theta Z^{n+1} + (1-\theta)Z^n$ for $Z = U, V, R, S, \bar{\Phi}, \bar{\bar{\Phi}}$, $Z^n \approx Z(t_n)$ and $0 \leq \theta \leq 1$, $n = 0, 1, \ldots N-1$. For $\theta = 1$ one obtain the fully implicit finite difference scheme, for $\theta = 0$ - explicit and for $\theta = 1/2$ - the Crank-Nicolson scheme. As we want to derive schemes of higher order, in the numerical experiments we use mainly $\theta = 1/2$. The numerical solution from previous time step $t = t_n$ is set as initial estimation for the following time step $t = t_{n+1}$. Then for finding the solution on $t = t_{n+1}$ the iterative process with appropriate stopping criteria is used:

$$\begin{cases} \Upsilon'(\overset{k}{W}{}^{n+1}) \overset{k}{\Delta} = -\Upsilon(\overset{k}{W}{}^{n+1}), \\ \overset{k+1}{W}{}^{n+1} = \overset{k}{W}{}^{n+1} + \overset{k}{\Delta}. \end{cases} \tag{36}$$

Here $\overset{k}{\Delta}$ is a vector of the increments and the Jacobian matrix $\Upsilon'(\overset{k}{W}{}^{n+1})$ for $\theta = 1/2$ is

$$\Upsilon'(\overset{k}{W}{}^{n+1}) = \frac{\partial \Upsilon}{\partial W} = \left(\begin{array}{cc} \frac{1}{\tau} I + \frac{1}{2}\bar{P} - \frac{1}{2}\frac{\partial R}{\partial U} & \frac{1}{2}\frac{\partial R}{\partial V} \\ \frac{1}{2}\frac{\partial S}{\partial U} & \frac{1}{\tau} I + \frac{1}{2}\bar{\bar{P}} - \frac{1}{2}\frac{\partial S}{\partial V} \end{array} \right) \Bigg|_{(U,V)=(\overset{k}{U},\overset{k}{V})}, \tag{37}$$

where I is the identity matrix and $\overline{P}$, $\overline{\overline{P}}$ - as defined by (33), (34). In the numerical experiments to solve the first line in (36) which is a linear system of $2(M_x - 1)(M_y - 1)$ equations we use the so called inexact Newton method, i.e. we solve this system approximately using the MatLab function bicgstab(l) (biconjugate gradients stabilized (l) method) that gives better results for our examples in sense of convergence of the inner iterations and the CPU time.

Richardson extrapolation

Richardson extrapolation is a powerful computational tool which can successfully be used in the efforts to improve the accuracy of the of the approximate solutions of the systems of partial differential equations (PDEs) obtained by finite difference methods.
Therefore, another way for obtaining the difference schemes of higher order is to use the Richardson extrapolation method. The main idea [?] is to solve the difference scheme on two or more consecutive meshes and then to combine the obtained numerical solutions with appropriate weights. Let us assume that $h_x = h_y = h$ and for the numerical solution on the n-th time layer the following expression is true:

$$U_h^\tau = U_{(i,j)}^n = u(x_i, y_j, t^n) + C_1 h^\sigma + \chi(h, \tau), \quad (x_i, y_j, t_n) \in \Omega_{h,\tau}, \tag{38}$$

where function $\chi(h, \tau)$ is a remainder term and C_1 does not depend on h_x, h_y and τ. If we want to eliminate the term $C_1 h^\sigma$, we do the following steps:

- solve the difference scheme on two consecutive meshes: coarse one $\Omega_{h,\tau}$ and fine one $\Omega_{h/2,\tau}$ and let the corresponding numerical solutions be U_h^τ and $U_{h/2}^\tau$;
- find the weights γ_1 and γ_2 from the system

$$\begin{aligned} \gamma_1 + \gamma_2 &= 1 \\ \gamma_1 + \frac{\gamma_2}{2^\sigma} &= 0 \end{aligned} \tag{39}$$

- obtain a new numerical solution on the coarse mesh

$$U_{extr} = \gamma_1 U_h^\tau + \gamma_2 U_{h/2}^\tau \qquad (x_i, y_j, t_n) \in \Omega_{h,\tau} \ . \tag{40}$$

From (39) we have for the case of central Crank-Nicolson Scheme ($\sigma = 2$) that the coefficients for the Richardson extrapolation are

$$\gamma_1 = -1/3 \qquad \gamma_2 = 4/3. \tag{41}$$

In the case of CFDS and Richardson Extrapolation ($\sigma = 4$) the corresponding weight coefficients are

$$\gamma_1 = -1/15 \qquad \gamma_2 = 16/15. \tag{42}$$

If in (38) the more detailed analysis of the LTE is done, then the prolongation of the idea of space-time RE can be applied.

We start with presenting CFDS on the 1D system of the following two equations:

$$\frac{\partial u}{\partial t} - a(x)\frac{\partial^2 u}{\partial x^2} + b(x)\frac{\partial u}{\partial x} = f(x, t, u, v), \quad \frac{\partial v}{\partial t} - c(x)\frac{\partial^2 v}{\partial x^2} + d(x)\frac{\partial v}{\partial x} = g(x, t, u, v) \ . \tag{43}$$

We introduce a standard mesh:

$$\Omega_h = \{x_i = ih, \quad i = 0, 1, \ldots, M, \quad h = 1/M\} \tag{44}$$

and the difference operators

$$\delta_x \varphi_i = (\varphi_{i+1} - \varphi_{i-1})/2h, \, \delta_x^2 \varphi_i = (\varphi_{i+1} - 2\varphi_i + \varphi_{i-1})/h^2 \tag{45}$$

for some mesh function φ_i, $i = 0, 1, \ldots, M$. Applying these operators to the elliptic part of the system one may obtain

$$-a_i \delta_x^2 u_i + b_i \delta_x u_i - e_{1,i} = f(x_i, t, u_i, v_i) - \frac{\partial u_i}{\partial t} \equiv F_i \tag{46a}$$

$$-c_i \delta_x^2 v_i + d_i \delta_x v_i - e_{2,i} = g(x_i, t, u_i, v_i) - \frac{\partial v_i}{\partial t} \equiv G_i, \tag{46b}$$

where the truncation errors may be expressed in the following form:

$$e_{1,i} = \frac{h^2}{12}\left(2b\frac{\partial^3 u}{\partial x^3} - a\frac{\partial^4 u}{\partial x^4}\right)\Bigg|_i + O(h^4) \quad e_{2,i} = \frac{h^2}{12}\left(2d\frac{\partial^3 v}{\partial x^3} - c\frac{\partial^4 u}{\partial x^4}\right)_i + O(h^4). \tag{47}$$

Differentiating (43) twice with respect to x we obtain

$$\begin{cases} a\dfrac{\partial^3 u}{\partial x^3} = \left(b - \dfrac{da}{dx}\right)\dfrac{\partial^2 u}{\partial x^2} - \dfrac{db}{dx}\cdot\dfrac{\partial u}{\partial x} - \dfrac{\partial F}{\partial x} \\ a\dfrac{\partial^4 u}{\partial x^4} - 2b\dfrac{\partial^3 u}{\partial x^3} = \left(2\dfrac{db}{dx} - \dfrac{d^2 a}{dx^2}\right)\dfrac{\partial^2 u}{\partial x^2} + \dfrac{d^2 b}{\partial x^2}\dfrac{\partial u}{\partial x} - \left(b + 2\dfrac{da}{dx}\right)\dfrac{\partial^3 u}{\partial x^3} - \dfrac{\partial^2 F}{\partial x^2}. \end{cases} \tag{48}$$

To increase the order of the error to $O(h^4)$ in (46a) we have used the fact that

$$\left(a\frac{\partial^4 u}{\partial x^4} - 2b\frac{\partial^3 u}{\partial x^3}\right)_i = - (\delta_x^2 a_i - \widetilde{a}_i(\delta_x a_i - b_i) - 2\delta_x b_i)\delta_x^2 u_i \tag{49}$$

$$+ (\delta_x b_i - \widetilde{a}_i . \delta_x c_i)\delta_x u_i - \delta_x^2 F_i + \widetilde{a}_i F_i + O(h^2),$$

where

$$\widetilde{a}_i = (b_i + 2\delta_x a_i)/a_i \quad i = 1, \ldots, M-1. \tag{50}$$

Let

$$\alpha_i = (\delta_x^2 a_i - \widetilde{a}_i(\delta_x a_i - b_i) - 2\delta_x b_i), \tag{51}$$

$$\widetilde{\alpha}_i = a_i + \frac{h^2}{12}\alpha_i, \tag{52}$$

$$\widetilde{\widetilde{\alpha}}_i = b_i + \frac{h^2}{12}(\delta_x^2 b_i - \widetilde{a}_i \delta_i b_i). \tag{53}$$

Now, let us define the following difference operators:

$$l_i^h = -\widetilde{\alpha}_i \delta_x^2 + \widetilde{\widetilde{\alpha}}_i\ \delta_x, \quad \nu_i^h = 1 + \frac{h^2}{12}(\delta_x^2 - \widetilde{a}_i \delta_x), \quad \mathcal{P}_i^h = 6h^2 l_i^h, \quad \mathcal{Q}_i^h = 6h^2 \nu_i^h\ . \tag{54}$$

Let also

$$P_1 = tridiag(p_{i,i-1}, p_{i,i}, p_{i,i+1}),\ Q_1 = tridiag(q_{i,i-1}, q_{i,i}, q_{i,i+1}) \tag{55}$$

be three diagonal matrix corresponding to $\mathcal{P}$, $\mathcal{Q}$ with elements

$$p_{i,i} = 12a_i + h^2\alpha, p_{i,i\pm1} = -6a_i \pm \widetilde{\alpha}_i - 0.5h^2\alpha, \tag{56}$$

$$q_{ii} = 5h^2 \quad q_{i,i\pm1} = 0.25h^2(2 \mp \widetilde{\alpha}_i h). \tag{57}$$

Finally, if $U_i \approx u(x_i, t)$, then the semidiscretization of (46a) to order $O(h^4)$ is as follows:

$$\mathcal{P}_i^h U_i = \mathcal{Q}^h F_i \ \ i = 1, \ldots, M-1 \ \text{ and } \ U_0 = \Psi(x_0)\ \ U_M = \Psi(x_M). \tag{58}$$

In a similar way we treat (46b). Analoguous to $\widetilde{a}_i$, α_i, $\widetilde{\alpha}_i$, $\widetilde{\widetilde{\alpha}}_i$, P_1 and Q_1 we define $\widetilde{c}_i$, β_i, $\widetilde{\beta}_i$, $\widetilde{\widetilde{\beta}}_i$, P_2 and Q_2, replacing $a \leftrightarrow c$ and $b \leftrightarrow d$.

Compact Difference Schemes - space discretization for 2D

In this section, just for clarity we describe the construction of the CFDS for 2D for the system of two equations (12a)-(12b).
In order to eliminate the terms of $\mathcal{O}(h_x^2 + h_y^2)$ in (23) we differentiate the equation (12a) twice with respect to x obtaining expressions for $\frac{\partial^3 u}{\partial x^3}$, $\frac{\partial^4 u}{\partial x^4}$, and twice with respect to y for $\frac{\partial^3 u}{\partial y^3}$, $\frac{\partial^4 u}{\partial y^4}$.
Let

$$\tilde{a}_{i,j} = (c_{i,j} + 2\delta_x a_{i,j})/a_{i,j}, \quad \tilde{b}_{i,j} = (d_{i,j} + 2\delta_y b_{i,j})/b_{i,j}, \quad (i,j) \in \Omega_h \ . \tag{59}$$

Let also

$$\alpha_{i,j} = a_{i,j} + \frac{h_x^2}{12}\left(\delta_x^2 a_{i,j} - \tilde{a}_{i,j}(\delta_x a_{i,j} - c_{i,j}) - 2\delta_x c_{i,j}\right) + \frac{h_y^2}{12}\left(\delta_y^2 a_{i,j} - \tilde{b}_{i,j}\delta_y a_{i,j}\right), \tag{60}$$

$$\beta_{i,j} = b_{i,j} + \frac{h_x^2}{12}\left(\delta_x^2 b_{i,j} - \tilde{a}_{i,j}\delta_x b_{i,j}\right) + \frac{h_y^2}{12}\left(\delta_y^2 b_{i,j} - \tilde{b}_{i,j}(\delta_y b_{i,j} - d_{i,j}) - 2\delta_y d_{i,j}\right), \tag{61}$$

$$\tilde{\alpha}_{i,j} = c_{i,j} + \frac{h_x^2}{12}\left(\delta_x^2 c_{i,j} - \tilde{a}_{i,j}\delta_x c_{i,j}\right) + \frac{h_y^2}{12}\left(\delta_y^2 c_{i,j} - \tilde{b}_{i,j}\delta_y c_{i,j}\right), \tag{62}$$

$$\tilde{\beta}_{i,j} = d_{i,j} + \frac{h_x^2}{12}\left(\delta_x^2 d_{i,j} - \tilde{a}_{i,j}\delta_x d_{i,j}\right) + \frac{h_y^2}{12}\left(\delta_y^2 d_{i,j} - \tilde{b}_{i,j}\delta_y d_{i,j}\right), \tag{63}$$

and

$$\theta_{i,j} = \frac{h_y^2}{12}c_{i,j} - \frac{h_x^2}{12}(2\delta_x b_{i,j} - \tilde{a}_{i,j}b_{i,j}), \quad \tilde{\theta}_{i,j} = \frac{h_x^2}{12}d_{i,j} - \frac{h_y^2}{12}(2\delta_y a_{i,j} - \tilde{b}_{i,j}a_{i,j}), \tag{64}$$

$$\gamma_{i,j} = \frac{h_x^2}{12}b_{i,j} + \frac{h_y^2}{12}a_{i,j}, \quad \tilde{\gamma}_{i,j} = \frac{h_x^2}{12}(2\delta_x d_{i,j} - \tilde{a}_{i,j}d_{i,j}) + \frac{h_y^2}{12}(2\delta_y c_{i,j} - \tilde{b}_{i,j}c_{i,j}). \tag{65}$$

Define the following difference operators

$$l^h_{i,j} = -\alpha_{i,j}\delta_x^2 - \beta_{i,j}\delta_y^2 + \tilde{\alpha}_{i,j}\delta_x + \tilde{\beta}_{i,j}\delta_y - \gamma_{i,j}\delta_x^2\delta_y^2 + \theta_{i,j}\delta_x\delta_y^2 + \tilde{\theta}_{i,j}\delta_x^2\delta_y + \tilde{\gamma}_{i,j}\delta_x\delta_y \quad (66)$$

$$\nu^h_{i,j} = 1 + \frac{h_x^2}{12}(\delta_x^2 - \tilde{a}_{i,j}\delta_x) + \frac{h_y^2}{12}(\delta_y^2 - \tilde{b}_{i,j}\delta_y). \quad (67)$$

Applying these operators to (12a) we have

$$l^h_{i,j}u_{i,j} = \nu^h_{i,j}(r_{i,j} - u_{t,i,j}) + \mathcal{O}(h_x^4 + h_x^2h_y^2 + h_y^4). \quad (68)$$

For convenience, we introduce also the operators

$$\bar{\mathcal{P}}^h_{i,j} = 6h_x^2 l^h_{i,j}, \quad \bar{\mathcal{Q}}^h_{i,j} = 6h_x^2\nu^h_{i,j}. \quad (69)$$

Let $\sigma = h_x/h_y$ be the ratio of the mesh sizes. Then

$$\bar{\mathcal{P}}^h_{i,j}u_{i,j} = \sum_{k_1=-1}^{1}\sum_{k_2=-1}^{1} p_{i,j}^{(k_1,k_2)}u_{i+k_1,j+k_2}, \quad (70)$$

$$\bar{\mathcal{Q}}^h_{i,j}u_{i,j} = \sum_{k_1=-1}^{1}\sum_{k_2=-1}^{1} q_{i,j}^{(k_1,k_2)}u_{i+k_1,j+k_2}, \quad (71)$$

where

$$
\begin{aligned}
p_{i,j}^{(\pm 1,-1)} &= -\frac{a_{i,j}+\sigma^2 b_{i,j}}{2} \pm \frac{1}{4}\left(c_{i,j}-\sigma^2(2\delta_x b_{i,j}-\tilde{a}_{i,j}b_{i,j}) \mp \sigma d_{i,j} \pm \frac{1}{\sigma}(2\delta_y a_{i,j}-\tilde{b}_{i,j}a_{i,j})\right) h_x \\
&\quad \mp \frac{1}{8}\left(\sigma(2\delta_x-\tilde{a}_{i,j}d_{i,j})+\frac{1}{\sigma}(2\delta_y c_{i,j}-\tilde{b}_{i,j}c_{i,j})\right) h_x^2, \\
p_{i,j}^{(\pm 1,1)} &= -\frac{a_{i,j}+\sigma^2 b_{i,j}}{2} \pm \frac{1}{4}\left(c_{i,j}-\sigma^2(2\delta_x b_{i,j}-\tilde{a}_{i,j}b_{i,j}) \pm \sigma d_{i,j} \mp \frac{1}{\sigma}(2\delta_y a_{i,j}-\tilde{b}_{i,j}a_{i,j})\right) h_x \\
&\quad \pm \frac{1}{8}\left(\sigma(2\delta_x-\tilde{a}_{i,j}d_{i,j})+\frac{1}{\sigma}(2\delta_y c_{i,j}-\tilde{b}_{i,j}c_{i,j})\right) h_x^2, \\
p_{i,j}^{(\pm 1,0)} &= \sigma^2 b_{i,j}-5a_{i,j} \pm \left(3\tilde{\alpha}_{i,j}-\frac{1}{2}c_{i,j}+\frac{\sigma^2}{2}(2\delta_x b_{i,j}-\tilde{a}_{i,j}c_{i,j})\right) h_x \qquad (72) \\
&\quad -\frac{1}{2}\left(\delta_x^2 a_{i,j}-\tilde{a}_{i,j}(\delta_x a_{i,j}-c_{i,j})-2\delta_x c_{i,j}+\frac{1}{\sigma^2}(\delta_y^2 a_{i,j}-\tilde{b}_{i,j}\delta_y a_{i,j})\right) h_x^2 \\
p_{i,j}^{(0,\pm 1)} &= a_{i,j}-5\sigma^2 b_{i,j} \pm \left(3\sigma\tilde{\beta}_{i,j}-\frac{\sigma}{2}d_{i,j}+\frac{1}{2\sigma}(2\delta_y a_{i,j}-\tilde{b}_{i,j}a_{i,j})\right) h_x \\
&\quad -\frac{1}{2}\left(\sigma^2(\delta_x^2 b_{i,j}-\tilde{a}_{i,j}\delta_x b_{i,j})+\delta_y^2 b_{i,j}-2\delta_y d_{i,j}-\tilde{b}_{i,j}(\delta_y b_{i,j}-d_{i,j})\right) h_x^2, \\
p_{i,j}^{(0,0)} &= 10(a_{i,j}+\sigma^2 b_{i,j})+\left(\delta_x^2 a_{i,j}-\tilde{a}_{i,j}(\delta_x a_{i,j}-c_{i,j})-2\delta_x c_{i,j}+\frac{1}{\sigma^2}(\delta_y^2 a_{i,j}-\tilde{b}_{i,j}\delta_y a_{i,j})\right) h_x^2 \\
&\quad +\left(\sigma^2(\delta_x^2 b_{i,j}-\tilde{a}_{i,j}\delta_x b_{i,j})+\delta_y^2 b_{i,j}-2\delta_y d_{i,j}-\tilde{b}_{i,j}(\delta_y b_{i,j}-d_{i,j})\right) h_x^2
\end{aligned}
$$

and

$$
q_{i,j}^{(\pm 1,\pm 1)}=0,\ q_{i,j}^{(\pm 1,0)}=\frac{1}{4}(2\mp\tilde{a}_{i,j}h_x)h_x^2,\ q_{i,j}^{(0,\pm 1)}=\frac{1}{4}(2\mp\frac{\tilde{b}_{i,j}}{\sigma}h_x)h_x^2,\ q_{i,j}^{(0,0)}=4h_x^2. \qquad (73)
$$

With these notations, after dropping the term $\mathcal{O}(h_x^4 + h_x^2 h_y^2 + h_y^4)$ in (68) the semi-discrete compact finite difference approximation of (12a) and (12b) and the left parts of (13), (14) are as follows:

$$\begin{cases} \bar{\mathcal{P}}^h_{i,j} u^h_{i,j} = \bar{\mathcal{Q}}^h_{i,j} \left(r^h_{i,j} - \frac{d}{dt} u^h_{i,j} \right), & (i,j) \in \Omega_h, \quad t \in (0,T], \\ u^h_{i,j} = \bar{\phi}_{i,j}, & (i,j) \in \partial\Omega_h, \quad t \in (0,T], \\ u^h_{i,j} = \bar{\psi}_{i,j}, & (i,j) \in \bar{\Omega}_h, \quad t = 0. \end{cases} \tag{74}$$

$$\begin{cases} \bar{\bar{\mathcal{P}}}^h_{i,j} v^h_{i,j} = \bar{\bar{\mathcal{Q}}}^h_{i,j} \left(s^h_{i,j} - \frac{d}{dt} v^h_{i,j} \right), & (i,j) \in \Omega_h, \quad t \in (0,T], \\ v^h_{i,j} = \bar{\bar{\phi}}_{i,j}, & (i,j) \in \partial\Omega_h, \quad t \in (0,T], \\ v^h_{i,j} = \bar{\bar{\psi}}_{i,j}, & (i,j) \in \bar{\Omega}_h, \quad t = 0. \end{cases} \tag{75}$$

Now we introduce the matrix representation for the system (74), (75). We obtain the following system of ordinary differential equations

$$\bar{Q} \frac{d}{dt} U^h + \bar{P} U^h = \bar{Q} R + \bar{\Phi}, \quad t \in (0,T], \tag{76}$$

$$\bar{\bar{Q}} \frac{d}{dt} V^h + \bar{\bar{P}} V^h = \bar{\bar{Q}} S + \bar{\bar{\Phi}} \tag{77}$$

with initial conditions $U^h(0)$ and $V^h(0)$ obtaining from $\bar{\psi}$ and $\bar{\bar{\psi}}$ for $(i,j) \in \Omega_h$ after the reordering. In system (76), (77) the matrix $\bar{P}$ (similarly $\bar{\bar{P}}$) is $(M_y - 1) \times (M_y - 1)$ block-tridiagonal matrix $\bar{P} = tridiag(\bar{P}_{k,k-1}, \bar{P}_{k,k}, \bar{P}_{k,k+1})$ and $\bar{P}_{k,l}$, $l = k-1, k, k+1$ are also tridiagonal matrices of order $(M_x - 1) \times (M_x - 1)$. Then from (72) the entries of $\bar{P}_{k,l}$, $\bar{Q}_{k,l}$ are

$$\bar{P}_{k,l} = tridiag(p^{(-1,\varepsilon)}_{k,2:M_x-1}, p^{(0,\varepsilon)}_{k,2:M_x}, p^{(1,\varepsilon)}_{k,1:M_x-2}) \qquad l = k + \varepsilon, \quad \varepsilon = 0, \pm 1 \,. \tag{78}$$

$$\bar{Q}_{k,l} = tridiag(q^{(-1,\varepsilon)}_{k,2:M_x-1}, \; q^{(0,\varepsilon)}_{k,2:M_x}, \; q^{(1,\varepsilon)}_{k,1:M_x-2}) \qquad l = k + \varepsilon, \quad \varepsilon = 0, \pm 1 \tag{79}$$

with a remark that for $\varepsilon = \pm 1$ matrixes $\bar{Q}_{k,l}$ are diagonal (instead tridiagonal) matrices, see (73). The vectors $\bar{\Phi}$ and $\bar{\bar{\Phi}}$ are associated with the boundary functions and also depend on time t.

Time discretization

For discretization of the ODE system (76)-(79) in time the θ-weight method with $\theta = 1/2$ is used in the numerical experiments. Then the Crank-Nicolson full discretization of (76), (77) is as follows:

$$\begin{aligned} \bar{Q}\frac{U^{n+1}-U^n}{\tau} + \bar{P}U^{n,\theta} &= \bar{Q}R^{n,\theta} + \bar{\Phi}^{n,\theta}, \quad n = 1, ..., N-1, \\ \bar{\bar{Q}}\frac{V^{n+1}-V^n}{\tau} + \bar{\bar{P}}V^{n,\theta} &= \bar{\bar{Q}}S^{n,\theta} + \bar{\bar{\Phi}}^{n,\theta}, \quad n = 1, ..., N-1. \end{aligned} \tag{80}$$

We apply the classical Newton method. The system (80) is rewritten in the form $\Upsilon(W) = 0$, where $W = [U^T, V^T]^T$ is a vector of length $2(M_x - 1)(M_y - 1)$. Similarly the numerical solution from previous time layer $t = t_n$ is set as initial estimation $\overset{0}{W}{}^{n+1}$ on the new time layer $t = t_{n+1}$. Then for finding the solution on $t = t_{n+1}$ it follows the iterative process, analogous to (36). Now, $\overset{k}{\Delta}$ is a vector of the increments and the Jacobian matrix $\Upsilon'(\overset{k}{W}{}^{n+1})$ for $\theta = 1/2$ is

$$\Upsilon'(\overset{k}{W}{}^{n+1}) = \left(\begin{array}{cc} \frac{1}{\tau}\bar{Q} + \frac{1}{2}\bar{P} - \frac{1}{2}\bar{Q}\frac{\partial R}{\partial U} & \frac{1}{2}\bar{Q}\frac{\partial R}{\partial V} \\ \frac{1}{2}\bar{\bar{Q}}\frac{\partial S}{\partial U} & \frac{1}{\tau}\bar{\bar{Q}} + \frac{1}{2}\bar{\bar{P}} - \frac{1}{2}\bar{\bar{Q}}\frac{\partial S}{\partial V} \end{array} \right) \Bigg|_{(U,V)=(\overset{k}{U},\overset{k}{V})}. \tag{81}$$

Example 1 (Test problem with known analytical solution)

We consider two examples to illustrate the properties of the numerical schemes derived. The first one is an artificial problem with analytical solution and the second one is the two dimensional air-pollution model described in Section 2.
Here we consider a problem slightly different from the problem (1)-(5), namely, we add the artificial source terms ξ_l, $l = 1, ..., 10$:

$$\frac{\partial u_l}{\partial t} - K\triangle u_l + \mathbf{b}_l.\nabla u_l = R_l(x, y, \mathbf{u}) + \xi_l(x, y, t), \quad (x, y, t) \in \Omega \times (0, T]. \tag{82}$$

The parameters are as follows: $X = Y = 500km$, $T = 1440min$, $K = 1.8$, $\mu = 2\pi/(60T)$, $\mathbf{b}_l = (\mu(y - Y/2), \mu(x - X/2))$.
We take as particular exact solution of (82) for $l = 1, ..., 10$ the functions

$$u_l(x, y, t) = U := \exp(-t/T)sin(\frac{\pi x}{X})sin(\frac{\pi y}{Y}), \quad (x, y, t) \in \overline{\Omega} \times [0, T]. \tag{83}$$

Then, the corresponding initial and boundary conditions are as follows:

$$u_l(x, y, 0) = U(x, y, 0) = \sin(\pi x/X)\sin(\pi y/Y), \quad (x, y) \in \overline{\Omega} = [0, X] \times [0, Y], \tag{84}$$

$$u_l(x, y, t) = U(x, y, t) = 0, \qquad (x, y) \in \partial\Omega, \quad t \in (0, T]. \tag{85}$$

Now, inserting (83) into (82), we calculate the residual functions ξ_l:

$$\xi_l(x, y, t) = f_{lin} + f_{n,l} \qquad l = 1, \ldots, 10, \tag{86}$$

where

$$f_{lin} = \Big(-1/T + (\pi^2/X^2 + \pi^2/Y^2)K \tag{87}$$

$$+\mu(y - Y/2)\pi/X \cot(\pi x/X) + \mu(x - X/2)\pi/Y \cot(\pi y/Y)\Big)\, U \tag{88}$$

and

$$f_{n,1} = -k_5 U + (k_6 + k_4 + k_3)U^2 \qquad f_{n,6} = -k_9 U^2$$

$$f_{n,2} = k_5 U - (k_6 + k_4 + k_3 - k_9)U^2 \qquad f_{n,7} = (-2k_2 - k_{10})U - (k_3 - k_4)U^2$$

$$f_{n,3} = k_1 U^2 \qquad f_{n,8} = (-4k_1 + k_3)U^2$$

$$f_{n,4} = k_2 U - (2k_1 + k_3)U^2 \qquad f_{n,9} = (-2k_8 + k_{10})U - (k_4 - k_1 + k_9)U^2$$

$$f_{n,5} = (k_7 - k_5)U + k_6 U^2 \qquad f_{n,10} = (-k_7 + k_8)U$$

The values of the coefficients k_l, $l = 1, \ldots, 10$ are taken from Table 3. For the l^{th} substances with $error_{M,l}$ we denote the error (the difference between the exact and the numerical solution) in maximum norm, obtained on the last time layer $t_N = T$ for the number of space subintervals $M_x = M_y = M$:

$$error_{M,l} = \max_{i,j \in \bar{\Omega}_h} \| u_l(x_i, y_j, t_N) - u_l^h(i, j, N) \|. \tag{89}$$

The ratio between the errors obtained on two consecutive mesh refinements (usually doubling) is denoted by *ratio*:

$$ratio = ratio_{M,l/2M,l} =: error_{M,l}/error_{2M,l}. \tag{90}$$

In the Table the mesh refinement analysis using CDS and CFDS is presented. The results confirm the theoretical rate of convergence, i.e. the ratio near four confirm the second order for the CDS and near sixteen - the fourth order for the CFDS. Also, as the CFDS has an error $O(h^4 + \tau^2)$, to observe the fourth order, when doubling the number of mesh points in space one must take quadruple mesh points in time. The *advantage* of the CFDS is corroborated by presenting the CPU time - there needs smaller time for the CFDS to obtain results with better accuracy in despite of the using of more time layers.

Table: Comparison of the maximum absolute errors of the CDS and CFDS with $M_x = M_y$ for **Example 1**

CDS, $O(h^2 + \tau^2)$					CFDS, $O(h^4 + \tau^2)$				
M_x	N	$error_M$	*ratio*	CPU	M_x	N	$error_M$	*ratio*	CPU
4	4	5.702 e-03	-	0.58	4	4	5.875 e-03	-	0.72
8	8	1.449 e-03	3.94	1.82	8	16	3.595 e-04	16.34	3.04
16	16	3.637 e-04	3.99	14.42	16	64	2.232 e-05	16.11	29.74
32	32	9.102 e-05	4.001	143.7	32	256	1.392 e-06	16.03	1076
64	64	2.276 e-05	4.00	3959	64	1024	8.698 e-08	16.003	60907
128	128	5.691 e-06	4.00	32709	128	4096	5.436 e-09	16.0001	720477

In the Table the mesh refinement analysis using CDS and CFDS with Richardson extrapolation in space (using corresponding weights from (41) and (42)) are presented. Again, to observe the fourth and the sixth order of CDSRE and CFDSRE, doubling mesh points in space one must take the number of time layers four and eight times more from the previous experiment. The results confirm the expected rates of convergence for both numerical methods. The ratio near 64 corresponds with the sixth order of the CFDSRE. Comparing of the CPU time of Table 4 and Table 5 shows a priority of using Richardson Extrapolation obtaining smaller errors for smaller computational time, nevertheless that the Richardson Extrapolation needs to compute the numerical solutions on two consecutive meshes. The *advantage* of CFDS with RE is also clearly seen.

Table: Comparison of the errors in maximum norm for the numerical **Example 1** for CDS and CFDS with Richardson extrapolation in space and $M_x = M_y$

CDS with RE in space, $O(h^4 + \tau^2)$					CFDS with RE in space, $O(h^6 + \tau^2)$				
M_x	N	err_N	ratio	CPU	M_x	N	err_N	ratio	CPU
4	4	5.677 e-03	-	1.34	4	4	5.711 e-03	-	1.38
8	16	3.545 e-04	16.014	16.17	8	32	8.912 e-05	64.087	17.45
16	64	2.216 e-05	15.997	544	16	256	1.392 e-06	64.022	1497
32	256	1.385 e-06	16.001	3055	32	2048	2.1757 e-08	63.989	23390

In the Table the mesh refinement analyses using CDS and CFDS with Richardson extrapolation in space and time are presented. Again, to observe the fourth and the sixth order of CDSRE and CFDSRE, doubling mesh points in space one must take the number of time layers two and eight times more from the previous experiment. This would cause to extremely growth of CPU time for the case of CFDS and therefore we take here four times (instead eight times) smaller mesh intervals in time. The results confirm the expected rates of convergence for both numerical methods. Comparing of the CPU time of Tables shows a *priority* of using Richardson Extrapolation both in space and time obtaining smaller errors for smaller computational time. The advantage of CFDSRE is also clearly seen.

Table: Comparison of the errors in maximum norm for the numerical **Example 1** for CDS and CFDS with Richardson extrapolation in space and time and $M_x = M_y$

CDS with RE in space and time, $O(h^4 + \tau^4)$					CFDS with RE in space and time $O(h^6 + \tau^4)$				
M_x	N	err_N	ratio	CPU	M_x	N	err_N	ratio	CPU
4	4	5.649 e-05	-	6.73	4	4	8.476 e-06	-	3.36
8	8	9.722 e-06	5.81	18.71	8	16	1.748 e-07	48.49	30.26
16	16	5.989 e-07	16.23	194.81	16	64	2.847 e-09	61.39	1276
32	32	3.715 e-08	16.12	4594	32	256	4.529 e-11	62.86	66991
64	64	2.171 e-09	16.03	37101	64	1024	7.086 e-13	63.91	790800

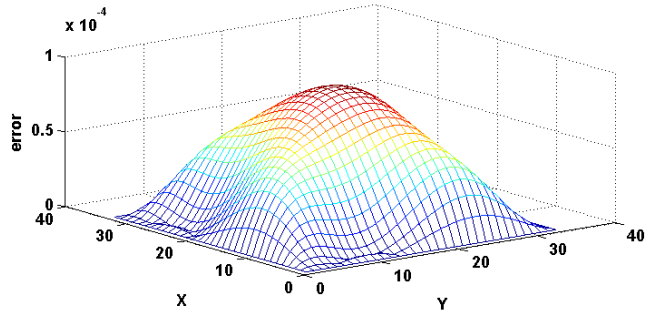

(a)

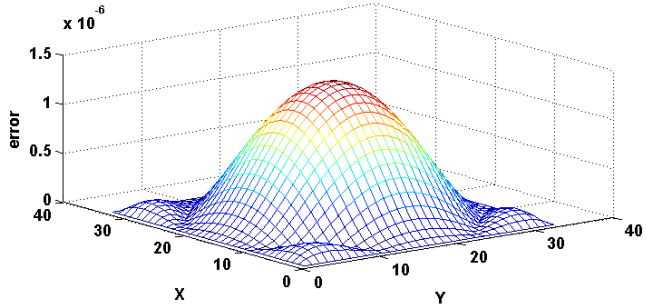

(b)

Fig 16: Error in maximum norm for the *Example 1*: (a) CDS with mesh parameters $M_X = M_y = 32$, $N = 32$; (b) CFDS for $M_X = M_y = 32$, $N = 256$

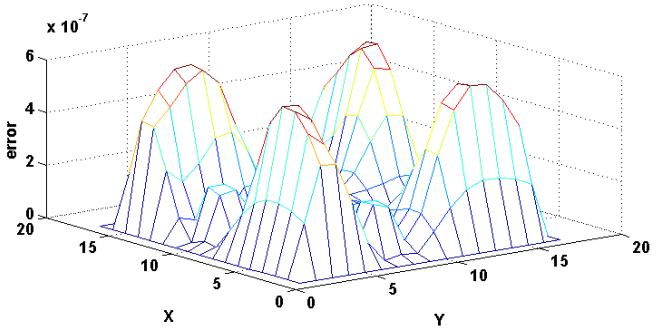

(a)

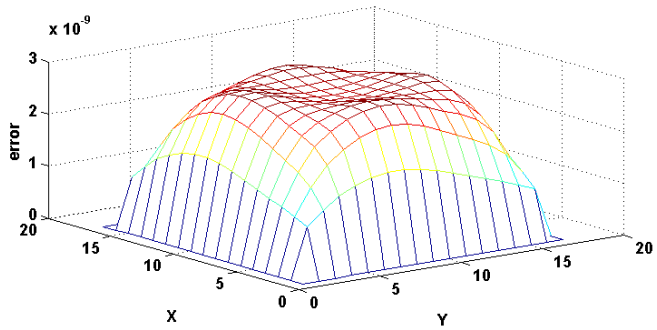

(b)

Fig 16: Error in maximum norm for *Example 1*: (a) CDS with RE in space and time $M_X = M_y = 16$, $N = 16$; (b) CFDS with RE in space and time $M_X = M_y = 16$, $N = 64$

Numerical example - Example 2 (unknown exact solution)

In this case we consider more realistic variant of problem (1)-(5) with the following parameters of the domain: the spatial domain is the square $\Omega = [0, 500]^2$ with side length 500 km, the length of the time interval $[0, T]$ is 1440 min and the number of equations is $L = 10$. The initial conditions on the time level $t = 0$ are the constant functions

$$\mathbf{u}_0(x, y) = (10^3, 10^3, 10^3, 5.10^3, 5.10^3, 10^2, 10^{-2}, 10^{-2}, 10^{-3}, 10^{-11}), \tag{91}$$

measured in mol/km^3 and the boundary conditions are chosen to be periodic: γ_i has the form

$$\gamma_l(t) = const_l(sin(t/C) + 2), \tag{92}$$

where $C = 4$ is a constant and the constants $const_l$, $l = 1, \ldots, L$ are chosen in such a way that the compatibility of the boundary and initial data is ensured. The diffusion coefficient is set to be $K = 1.8km^2/min$ and the coefficient μ is $\mu = 2\pi/(60 * T)$.
In this example there is no analytical solution. One way of calculating the convergence rate is the method of Runge on three nested meshes. Here we use another idea. As an "exact" solution we take the solution, obtained with a "least" mesh size in space. In the following tables we denote these solutions by **bold** font. Also in this case we present the relative error in maximum norm. We control the rate of convergence denoted by *order* and evaluated by

$$order = log_2(ratio) \tag{93}$$

when doubling the number of mesh points and in other case

$$order = log(error_{M',l}/error_{M'',l})/log(M''/M') \tag{94}$$

where M' and M'' are two consecutive numbers of mesh points in space in the mesh refinement analysis.

In Table we present the results obtained by CDS with number of time steps $N = 256$ for the first and fifth substances u_1 and u_5 at the central node with coordinates $(x_{M/2}, y_{M/2}) = (X/2, Y/2) = (250, 250)$. The second order is confirmed. It is interesting to note that neverthelees u_1 and u_5 have different values, the relative errors are approximately the same for the both pollutants. Similar results are presented in Table, but at the point $(x, y) = (X/6, Y/6) = (83.33, 83.33)$. Again the second order of the CDS can be seen.

Table: The rate of convergence for the **Example 2** for the CDS at the central node $(x, y) = (X/2, Y/2)$ with time steps $N = 256$ for the first and fifth substances u_1 and u_5

U_1					U_5				
M_x	M_y	numerical value	rel. error	order	M_x	M_y	numerical value	rel. error	order
8	8	1975.882481	1.001 e-02	-	8	8	4523.292977	1.001 e-03	-
16	16	1991.143607	2.366 e-03	2.08	16	16	4558.229378	2.366 e-03	2.08
24	24	1993.813011	1.028 e-03	2.05	24	24	4564.340280	1.028 e-03	2.05
32	32	1994.730617	5.685 e-04	2.06	32	32	4566.440899	5.684 e-04	2.06
40	40	1995.152323	3.572 e-04	2.08	40	40	4567.406285	3.572 e-04	2.08
48	48	1995.380607	2.428 e-04	2.11	48	48	4567.928881	2.428 e-04	2.11
56	56	1995.517989	1.739 e-04	2.16	56	56	4568.243380	1.740 e-04	2.16
64	64	1995.607048	1.293 e-04	2.21	64	64	4568.447260	1.293 e-04	2.21
192	192	**1995.865185**			192	192	**4569.038195**		

Table: The numerical values, the relative errors and the rate of convergence for **Example 2** by the CDS at the node $(x, y) = (X/6, Y/6)$ with number of time steps $N = 256$ for the first and fifth substances u_1 and u_5

U_1					U_5				
M_x	M_y	numerical value	rel. error	order	M_x	M_y	numerical value	rel. error	order
6	6	1068.473273	4.271 e-02	-	6	6	2447.733406	4.203 e-02	-
12	12	1110.557284	5.007 e-03	3.09	12	12	2542.369591	4.998 e-03	3.07
24	24	1115.537216	5.451 e-04	3.19	24	24	2553.746683	5.450 e-04	3.20
48	48	1116.056372	7.994 e-05	2.76	48	48	2554.935074	7.992 e-05	2.77
96	96	1116.145593	1.783 e-05	2.16	96	96	2555.139279	1.782 e-05	2.16
192	192	**1116.165491**	-		192	192	**2555.184819**	-	

With the same parameters the experiments are repeated using CFDS. The results are presented in Tables. The fourth order in both cases (central node (x,y)=(X/2,Y/2) and node (x,y)=(X/6,Y/6)) for the both substances u_1 and u_5 is confirmed. Again at the central node the relative errors are likely the same.

Table: The rate of convergence for **Example 2** for the CFDS at the central node $(x, y) = (X/2, Y/2)$ with number of time steps $N = 256$ for the first and fifth substances u_1 and u_5

U_1					U_5				
M_x	M_y	numerical value	rel. error	order	M_x	M_y	numerical value	rel. error	order
8	8	2000.633296	2.273 e-03	-	8	8	4580.154033	2.417 e-03	-
16	16	1996.195827	1.495 e-04	3.988	16	16	4569.795122	1.495 e-04	4.014
24	24	1995.956736	2.972 e-05	3.984	24	24	4569.247779	2.972 e-05	3.984
32	32	1995.916219	9.419 e-06	3.994	32	32	4569.155025	9.420 e-06	3.994
40	40	1995.905118	3.858 e-06	4.000	40	40	4569.129612	3.858 e-06	4.000
48	48	1995.901126	1.858 e-06	4.008	48	48	4569.120473	1.858 e-06	4.008
56	56	1995.899414	9.997 e-07	4.019	56	56	4569.116553	9.997 e-07	4.019
64	64	1995.898582	5.831 e-07	4.037	64	64	4569.114649	5.831 e-07	4.037
192	192	**1995.897418**			192	192	**4569.112120**		

Table: The rate of convergence of the CFDS for **Example 2** at the node $(x, y) = (X/6, Y/6)$ with number of time steps $N = 256$ for the first and fifth substances u_1 and u_5

U_1					U_5				
M_x	M_y	numerical value	rel. error	order	M_x	M_y	numerical value	rel. error	order
6	6	1043.293291	6.529 e-02	-	6	6	2257.948316	1.163 e-01	-
12	12	1118.080459	1.710 e-03	5.25	12	12	2550.112259	1.991 e-03	5.86
24	24	1116.078012	8.411 e-05	4.34	24	24	2554.999291	7.834 e-05	4.66
48	48	1116.166054	5.229 e-06	4.00	48	48	2555.186084	5.236 e-06	3.91
96	96	1116.171550	3.054 e-07	4.09	96	96	2555.198680	3.068 e-07	4.09
192	192	**1116.171891**	-		192	192	**2555.199463**	-	

In Tables the results obtained by the CDSRE and CFDSRE in space are shown. The number of time layers are $N = 256$ and the presented values are the numerical values at the last time layer $t_N = T$ at the central node $(x, y) = (X/2, Y/2)$. The results confirm the fourth order for the CDSRE and the sixth order for CFDSRE.

Table: The rate of convergence for **Example 2** for the CDS with RE in space at the central node $(x, y) = (X/2, Y/2)$ with time steps $N = 256$

U_1					U_5				
M_x	M_y	numerical value	rel. error	order	M_x	M_y	numerical value	rel. error	order
8	8	1996.230649	1.669 e-04	-	8	8	4569.874845	1.669 e-04	-
16	16	1995.926287	1.446 e-05	3.529	16	16	4569.178073	1.446 e-05	3.529
24	24	1995.903139	2.862 e-06	3.995	24	24	4569.125081	2.863 e-06	3.994
32	32	1995.899192	8.856 e-07	4.079	32	32	4569.116047	8.855 e-07	4.078
40	40	1995.898128	3.524 e-07	4.129	40	40	4569.113611	3.524 e-07	4.129
48	48	1995.897751	1.632 e-07	4.225	48	48	4569.112746	1.631 e-07	4.224
56	56	1995.897590	8.268 e-08	4.409	56	56	4569.112378	8.267 e-08	4.409
64	64	1995.897512	4.386 e-08	4.748	64	64	4569.112201	4.385 e-08	4.749
96	96	**1995.897425**			96	96	**4569.112001**		

Table: The rate of convergence for **Example 2** for CFDS with RE in space for the central node $(x, y) = (X/2, Y/2)$ with time steps $N = 256$

U_1					U_5				
M_x	M_y	numerical value	rel. error	rate	M_x	M_y	numerical value	rel. error	rate
8	8	1995.899995	1.299 e-06	-	8	8	4569.104528	1.624 e-06	-
16	16	1995.897579	8.779 e-08	3.887	16	16	4569.112352	8.767 e-08	4.212
24	24	1995.897419	7.582 e-09	6.040	24	24	4569.111986	7.565 e-09	6.042
32	32	1995.897406	1.300 e-09	6.077	32	32	4569.111957	1.311 e-09	6.092
40	40	1995.897404	3.428 e-10	6.041	40	40	4569.111953	3.380 e-10	6.075
48	48	1995.897404	1.144 e-10	6.018	48	48	4569.111952	1.115 e-10	6.080
56	56	1995.897404	4.505 e-11	6.045	56	56	4569.111952	4.326 e-11	6.144
64	64	1995.897404	1.968 e-11	6.204	64	64	4569.111952	1.855 e-11	6.339
96	96	**1995.897404**			96	96	**4569.111952**		

In Figure the log-log plot of the errors versus space mesh size for the *Example 2* is presented, obtained by: CDS - red line, $-\star-$; CFDS - magenta line, $-\blacksquare-$; CDSRE - green line, $-\blacklozenge-$; CFDSRE in space - blue line, $-\bullet-$. The increasing of the slope of the lines corresponds with the increasing of the rate of convergence. The lowest line confirms the advantage of the CFDS in combination with Richardson extrapolation.

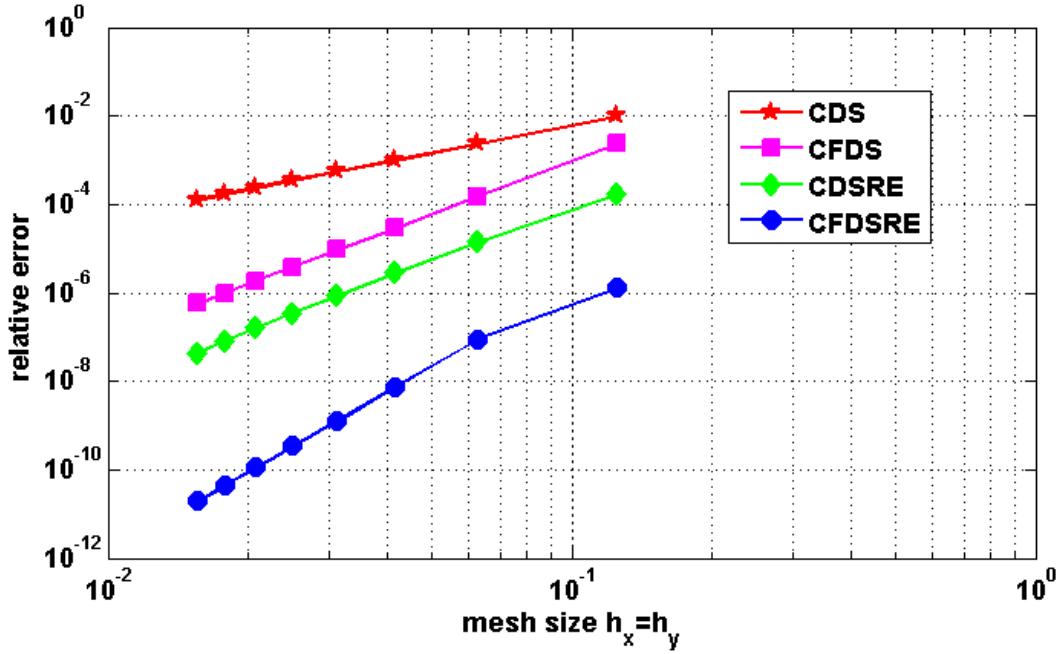

Fig 17: The log-log plot of the errors versus space mesh size for the *Example 2*, obtained by: CDS - red line, $-\star-$; CFDS - magenta line, $-\blacksquare-$; CDSRE - green line, $-\blacklozenge-$; CFDSRE in space - blue line, $-\bullet-$.

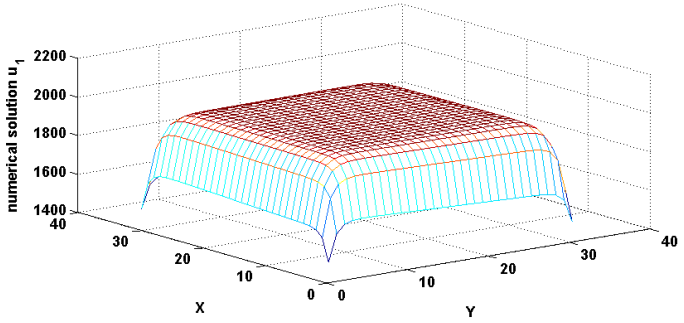

(a)

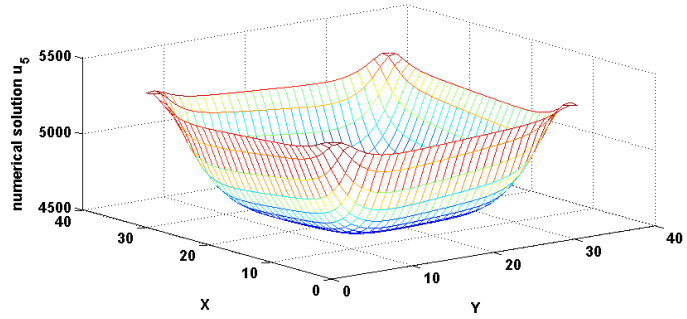

(b)

Fig 19: Numerical solution obtained with CDS for $\mu = 2\pi/(60\,T)$ with mesh parameteres $M_x = M_y = 32$, $N = 256$ for *Example 2*: (a) for u_1; (b) for u_5

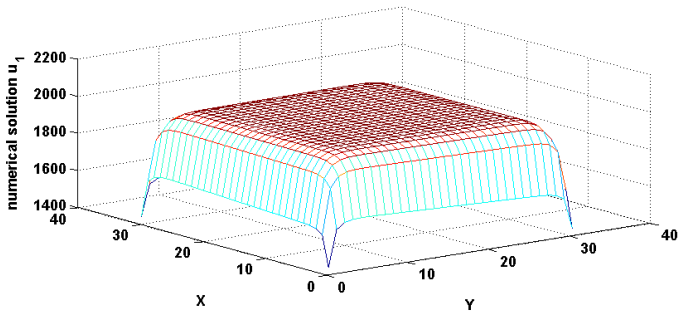

(a)

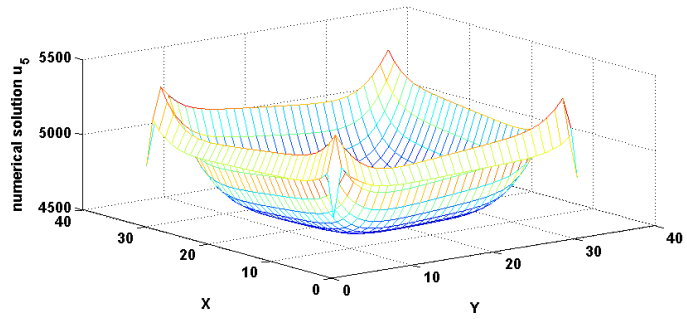

(b)

Fig 19: Numerical solution obtained with CFDS for $\mu = 2\pi/(60\,T)$ with mesh parameteres $M_x = M_y = 32$, $N = 256$ for *Example 2*: (a) for u_1; (b) for u_5

Many others experiments have been done. It is interesting to see the behaviour of the solutions if the coefficient μ in the convection term is taken to be $\mu = 2\pi/(X)$ as it is in paper of Karatson and Kuric instead $\mu = 2\pi/(60 * T)$ as it is in the paper of Georgiev and Zlatev. The increasing of the convective coefficients leads to significant change of the numerical solution near the corners. It can be seen that the constant initial values have been left relatively intact in the middle of the domain, but they have been stretched near the boundary by the sinusoidal boundary conditions.

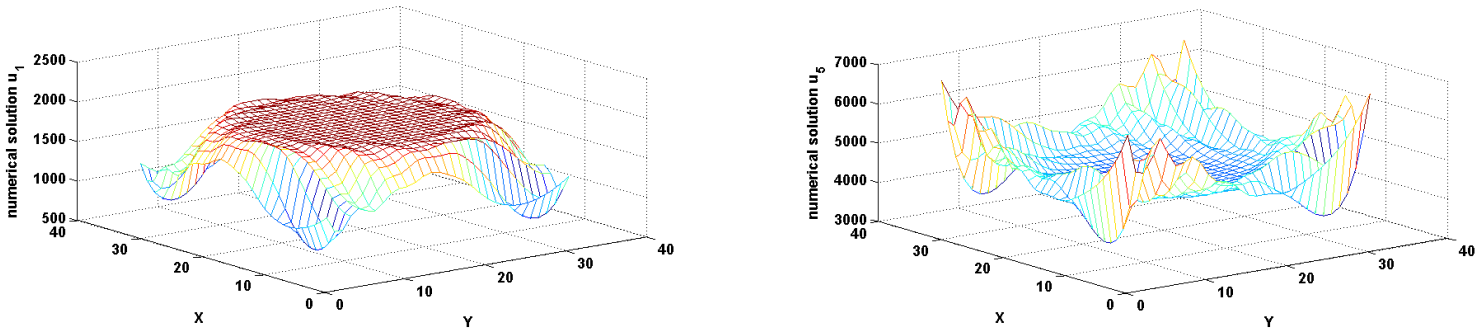

(a) (b)

Fig 20: Numerical solution for *Example 2*, obtained with CFDS for $\mu = 2\pi/500$ and $M_x = M_y = 32$, $N = 256$: (a) for u_1; (b) for u_5.

In Table the average number of iterations for *Example 1* at the outer (Newton) and at the inner (bicgstabl) part of the inexact Newton method for CDS and CFDS are presented. To go from the n-th time layer to the next $n+1$-th time layer we need of approximately three iterations at the outer (Newton) part for the both difference schemes. At the inner (bicgstabl) part for the case of CDS we need of three iterations and for the case of CFDS we observe the decreasing of the number of iterations from 3.40 to 2.05 when the numbers of the mesh points in space and time are increasing.

Table: The average number of iterations for *Example 1* at the outer (Newton) and inner (bicgstabl) parts of the inexact Newton method for CDS and CFDS

CDS					CFDS				
M_x	M_y	N	Newton	bicgstabl	M_x	M_y	N	Newton	bicgstabl
8	8	8	3	2.67	8	8	16	3	3.40
16	16	16	3	2.67	16	16	64	2.98	2.57
32	32	32	3	2.67	32	32	256	2.96	2.15
64	64	64	2.95	3.31	64	64	1024	2.65	2.05

Similar results are presented in Table 14 for *Example 2* obtained with the number of time steps $N = 256$. The number of the outer iterations is three for CDS and decreases from 3.80 to 3.17 for CFDS. In the opposite the number of the inner (bicgstabl) iterations increases for CDS from 1.75 to 6.54 and decreases from 4.70 to 2.50 for CFDS as a result of better local approximation.

Table: The number of average iterations for *Example 2* on the outer (Newton) and inner (bicgstabl) part of the inexact Newton method for CDS and CFDS with the number of time steps $N = 256$

CDS				*CFDS*			
M_x	M_y	Newton	bicgstabl	M_x	M_y	Newton	bicgstabl
8	8	3	1.75	8	8	3.80	4.70
16	16	3	2.48	16	16	3.96	4.36
32	32	3	3.86	32	32	3.32	3.67
64	64	3	6.54	64	64	3.17	2.50

In spite of all advantages of CFDS in sense of accuracy and CPU time, there is also some disadvantages. The stencil of the CFDS is nine-point and the sign condition of the discrete maximum principle is not fulfill. As a result the positivity of the numerical solution is break for some values of the mesh parameters in space ant time. In Figure the numerical solution for the pollutant NO_2 (u_2) for *Example 2* when $\mu = 2\pi/(T)$ and $M_x = M_y = 8$, $N = 256$, obtained by (a) CDS and by (b) CFDS is presented. The CDS preserves the positivity of the numerical solution, while the CFDS does not - near the corners the numerical solution is negative and has no chemical sense. This fact confirm, that the proposed methods needs of more careful analysis.

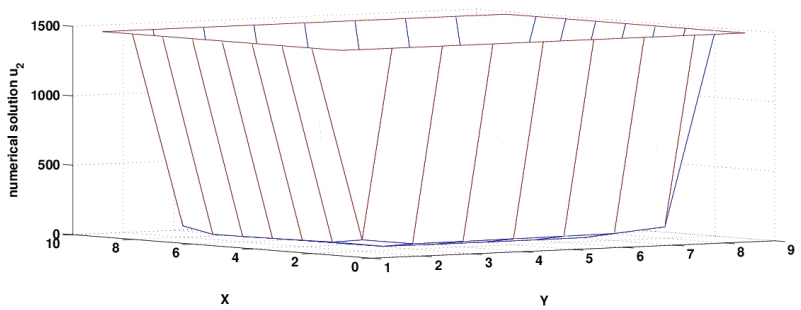

(a)

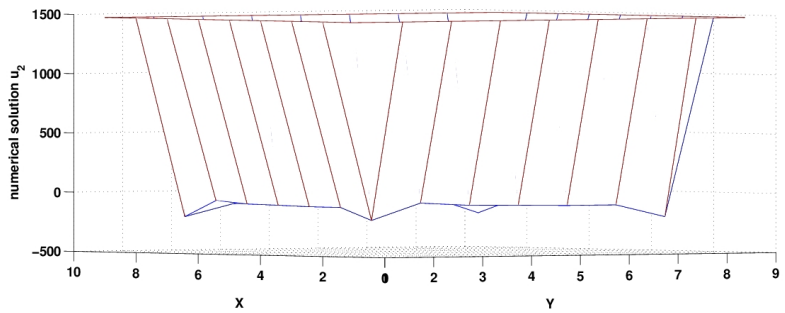

(b)

: Numerical solution for NO_2 - u_2 for $\mu = 2\pi/(T)$ with mesh parameters $M_x = M_y = 8$, $N = 256$ *Example 2*, obtained with: (a) CDS; (b) CFDS

Atmosphere model based on Chapman's cycle

We concentrate on the system (1)-(3) for $L = 3$ with coefficients, reaction and source terms that correspond to the atmosphere model based on Chapman's cycle. While a realistic atmospheric/air-pollution model main contain dozens of reacting species, our simple model capture the basic features of the complete practical models and the methods developed in the paper are already implemented to the model of the equations solved in previous papers.
The components of the system are the oxide (NO), nitrogen dioxide (NO_2) and ozone (O_3) denoted by u_1, u_2, u_3 respectively:

$$R_l(\mathbf{u}) = -r(\mathbf{u}), \quad l = 1, 3, \quad R_2(\mathbf{u}) = r(\mathbf{u}), \quad r(\mathbf{u}) = k_1 u_1 u_3 - k_2 u_2, \tag{95}$$

where k_1, k_2 are the forward and backward reaction rates.

Exact analytical sol. and Problem with Delta source terms

. Here we consider a problem slightly different from the problem (1)-(3):

$$\frac{\partial u_l}{\partial t} - K\triangle u_l + \mathbf{b}_l.\nabla u_l = R_l(x,y,\mathbf{u}) + \xi_l(x,y,t), (x,y,t) \in \Omega \times (0,T]. \tag{96}$$

The functions ξ_l, $l = 1,2,3$, and the initial and boundary conditions are chosen so that the exact solution is

$$u_l = \exp(-t)sin(\pi x)sin(\pi y), \quad l = 1,2, \quad (x,y,t) \in \overline{\Omega} \times [0,T], \tag{97}$$

$$u_3 = 1 + \exp(-t)sin(\pi x)sin(\pi y), \quad (x,y,t) \in \overline{\Omega} \times [0,T]. \tag{98}$$

The other parameters are as follows: $\overline{\Omega} = [0,1] \times [0,1]$, $T = 1$, $b_l = (0.1, 0.1)$, for $l = 1,2,3$, $K_1 = 1$, $K_2 = K_3 = 5$.
For the l^{th} substances with $error_{M,l}$ we denote the error (the difference between the exact and the numerical solution) in maximum norm, obtained on the last time layer $t_N = T$ for the number of space subintervals $M_x = M_y = M$:

$$error_{M,l} = \max_{i,j \in \bar{\Omega}_h} \|u_l(x_i, y_j, t_N) - u_l^h(i,j,N)\|. \tag{99}$$

The ratio between the errors obtained on two consecutive mesh refinements (usually doubling) is denoted by *ratio*:

$$ratio = ratio_{M,l/2M,l} =: error_{M,l}/error_{2M,l}. \tag{100}$$

In this example we consider problem (96), where functions ξ_l now are point source terms of the form

$$\xi_l(x,y,t) = f_l(t)\delta(x - \overline{x}_l, y - \overline{y}_l), \quad l = 1,2,3. \tag{101}$$

The parameters are as follows: $\overline{\Omega} = [0,1] \times [0,1]$, $T = 1$, $b_l = (-0.1, 0)$, for $l = 1,2,3$, $K_1 = 1$, $K_2 = K_3 = 5$, $k_1 = 1000$, $k_2 = 2000$, $(\overline{x}_1, \overline{y}_1) = (0.5, 0.5)$, $(\overline{x}_2, \overline{y}_2) = (0.25, 0.25)$, $(\overline{x}_3, \overline{y}_3) = (0.75, 0.75)$, $f_1(t) = 7$, $f_2(t) = 11$, $f_3(t) = 13$.

Table: Rel. error for the first species

CDS $O(h^2+\tau^2)$						CDS RE $O(h^4+\tau^2)$					
M_1	M_2	N	err_N	ratio	CPU	M_1	M_2	N	err_N	ratio	CPU
8	8	8	1.025e-03		1.46	8	8	8	1.820e-06		3.08
16	16	16	2.567e-04	3.991	3.33	16	16	16	1.814e-07	10.03	20.70
32	32	32	6.421e-05	3.998	20.48	32	32	32	1.219e-08	14.88	477
64	64	64	1.605e-05	3.999	442	64	64	64	7.642e-10	15.95	9871

Table 45: Rel. error for the first species

CFDS $O(h^4+\tau^2)$						CFDS RE $O(h^6+\tau^2)$					
M_1	M_2	N	err_N	ratio	CPU	M_1	M_2	N	err_N	ratio	CPU
8	8	8	5.223e-06		1.34	8	8	8	2.512e-09		2.95
16	16	32	3.293e-07	15.86	15.26	16	16	32	3.945e-11	64.31	38.27
32	32	128	2.062e-08	15.972	84.87	32	32	128	6.145e-13	64.19	373
64	64	512	1.289e-09	15.991	6384	64	64	512	9.598e-15	64.03	15510

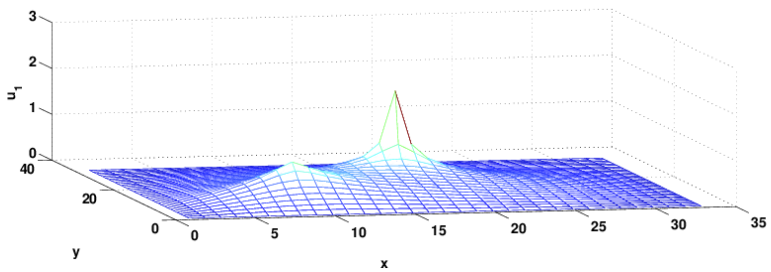

(a)

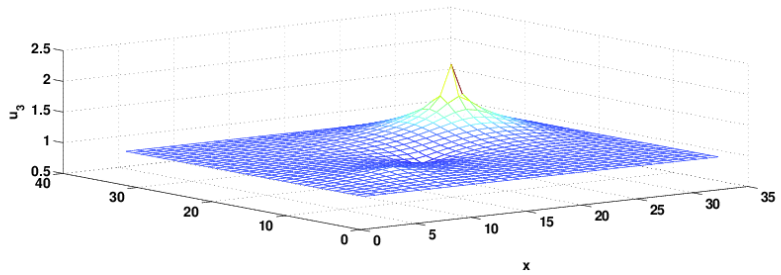

(b)

Fig 22: Numerical solution for the mesh with parameters $M_x = M_y = 32$, $N = 256$ for *Example 2*: (a) for *NO* - u_1; (b) for O_3 - u_3

- Two different ways for derivation of high-order difference schemes for semilinear parabolic systems of equations are analyzed.
- First, using central difference approximation with Richardson extrapolation the fourth-order method is obtained.
- Second, starting from CDS and following the method of auxiliary relations yielded from the original differential equations we constructed the fourth-order CFDS for semilinear parabolic systems with variable coefficients.
- Then, applying Richardson extrapolation to these CFDS we obtain the sixth-order approximations of the differential problems.
- The time-stepping is realized using θ-scheme, but in the numerical computations - by the Crank-Nicolson/Newton algorithm.
- The reported computational results demonstrate that the convergence rate of the CDS is $O(h^2 + \tau^2)$ and of the CFDS it is $O(h^4 + \tau^2)$, but in combination with Richardson extrapolation they are respectively $O(h^4 + \tau^2)$ and $O(h^6 + \tau^2)$.
- Considering Tables we can conclude the following: first is that for achieving the same accuracy, for example $\approx e - 06$ the CPU time of CDS is thirty times of the CPU time of CFDS, i.e. CFDS-method is much more faster. Second, taking in Tables for reference accuracy $\approx e - 06$ we conclude that CFDSRE are approximately two times faster than CDSRE. Third, taking in Tables 4,5 for reference accuracy $\approx e - 08$ CFDSRE is 2.6 times faster than CFDS.
- Numerically it is confirmed the advantages of the CFDS over the CDS both in the accuracy and CPU time. The skilfully application of Richardson extrapolation also plays important role in obtaining good results in real time with a small number of grid nodes despite the large intervals of the domain both in space and time in air pollution problems.
- In the next study we will present a theoretical analysis of the present approximation. Also, we will develop two-grid algorithms for solution of the corresponding nonlinear systems of algebraic equation.

ACKNOWLEDGMENTS

This research was supported by: EBR Hungary-Bulgaria

THANK YOU VERY MUCH FOR YOUR ATTENTION!